https://doi.org/10.5194/hess-2021-75
Preprint. Discussion started: 26 February 2021

Hydrology and Earth System Sciences
Open Access
Discussions

River-enhanced non-linear overtide variations in river estuaries

Leicheng Guo[1, *], Chunyan Zhu [1, 2], Huayang Cai [3], Zheng Bing Wang [1, 2, 4], Ian Townend [5], Qing He [1]

[1] State Key Lab of Estuarine and Coastal Research, East China Normal University, Shanghai 200241, China

[2] Department of Hydraulic Engineering, Faculty of Civil Engineering and Geosciences, Delft University of Technology, Delft 2600GA, the Netherlands

[3] School of Marine Engineering and Technology, Sun Yat-Sen University, Guangzhou, China

[4] Marine and Coastal Systems Department, Deltares, Delft 2629 HV, the Netherlands

[5] School of Ocean and Earth Sciences, University of Southampton, Southampton, UK

* *Corresponding author*, E-mail: lcguo@sklec.ecnu.edu.cn

Abstract: Tidal waves traveling into estuaries are modulated in amplitude and shape due to bottom friction, funneling planform and river discharge. The role of river discharge on damping incident tides has been well-documented, whereas our understanding of the impact on overtide is incomplete. Inspired by findings from tidal data analysis, in this study we use a schematized estuary model to explore the variability of overtide under varying river discharge. Model results reveal significant M_4 overtide generated inside the estuary. Its absolute amplitude decreases and increases in the upper and lower parts of the estuary, respectively, with increasing river discharge. The total energy of the M_4 tide integrated throughout the estuary reaches a transitional maximum when the

https://doi.org/10.5194/hess-2021-75
Preprint. Discussion started: 26 February 2021

river discharge to tidal mean discharge (R2T) ratio is close to unity. We further identify that the quadratic bottom stress plays a dominant role in governing the M_4 variations through strong river-tide interaction. River flow enhances the effective bottom stress and dissipation of the principal tides, and reinforces energy transfer from principal tide to overtide. The two-fold effects explain the nonlinear M_4 variations and the intermediate maximum threshold. The model results are consistent with data analysis in the Changjiang and Amazon River estuaries and highlight distinctive tidal behaviors between upstream tidal rivers and downstream tidal estuaries. The new findings inform study of compound flooding risk, tidal asymmetry, and sediment transport in river estuaries.

Key words: River discharge; Overtide; Bottom stress; Estuary

1. Introduction

Tides are a primary force driving water motion and transport of sediment and contaminant in estuarine and coastal environments. Examination of tidal wave dynamics supports many aspects of coastal management, including flooding risk mitigation, coastal erosion defense, and wetland conservation. Tidal dynamics in oceanic and coastal waters have been extensively studied for centuries (Green, 1837; Talke and Jay, 2020). It is already well established that tidal waves traveling into estuaries are altered in amplitude and shape due to water depth changes, channel convergence (Jay, 1991; Friedrichs and Aubrey, 1994; Lanzoni and Seminara, 1998; Talke and Jay, 2020), and river discharge (Godin, 1985; Horrevoets et al., 2004; Cai et al., 2014). Given tidal wave celerity is a function of water depth in shallow environments, high water travels faster than low water, leading to shorter rising tide and longer falling tide, i.e., tidal wave deformation and tidal asymmetry. Tidal wave deformation at the daily time scale is nicely represented by superimposition of M_2 and its first overtide M_4 (Pugh, 1987). The amplitude of M_4 overtide is basically small and insignificant in relatively deep and open coastal seas, but may become profound inside tidal estuaries. The energy of M_4 overtide inside estuaries is extracted from astronomical tides through the nonlinear processes (Parker, 1984; Talke and Jay, 2020). The behavior and dynamics of M_4 tide in tide-dominant estuaries and lagoons have been extensively examined because the resultant tidal asymmetry controls tide-averaged sediment transport and morphological changes (Parker, 1984; Speer and Aubrey, 1985; Friedrichs and Aubrey, 1988; Le Provost, 1991 etc.).

River flow enhances tidal energy dissipation and stimulates wave deformation (Jay and Flinchem, 1997; Godin, 1999; Horrevoets et a., 2004; Toffolon and Savenije, 2011). River discharge reinforces wave deformation by prolonging falling tides and shortening rising tides, which is featured by larger overtide amplitude under higher river discharge (Stronach and Murty, 1989; Gallo and Vinzon, 2005). However, a small number of studies suggest that the impact of river flow on tidal wave deformation and overtide generation exhibits more spatial variability within river estuaries under varying river discharge. For instance, Godin (1985, 1999) reported accelerated low water and retarded high water in the upper Saint Lawrence Estuary under larger river discharge, whereas the high water is hastened and the low water delayed in the lower part of the estuary. In the Changjiang River estuary, the amplitude of the quarter-diurnal tidal species (overtides and compound tides), resolved by continuous wavelet transform method, becomes larger in the lower part of the estuary, but smaller in the upper part of the estuary under high river flow conditions (Guo et al., 2015). These findings imply that the M_4 overtide is sensitive to river discharge magnitude and it displays different spatial variations under different river discharge conditions, which is, however, insufficiently understood.

The overtide generated locally within estuaries is inherently related to the nonlinear dynamics in shallow waters. Non-linearity enters the mathematical representation of a tidal system through the divergence of excess volume in the continuity equation and the advection and bottom friction terms in the momentum equation (Speer and Aubrey, 1985; Parker, 1984, 1991; Wang et al.

https://doi.org/10.5194/hess-2021-75
Preprint. Discussion started: 26 February 2021

1999, 2002). Pioneering studies with scaling analysis suggested that the advection term is insignificant when scaled with estuarine length or wavelength in short and tide-dominated estuaries, thus was ignored in past analytical study of tides (Speer and Aubrey, 1985; Friedrichs and Aubrey, 1994). However, in the presence of a river flow, the advection term may play a role in slowing down incident tidal waves and speeding up the reflected waves (Godin, 1985, 1991; van Rijn, 2011; Kästner et al., 2019). This is because river flow enlarges the mean current, therefore the advection term becomes significant and cannot be ignored in river estuaries (Talke and Jay, 2020). Parker (1984) provided a thorough analysis of the importance of frictional effects on tidal interactions. The quadratic bottom shear stress has the effect of reducing tidal amplitudes and decreasing wave celerity (Proudman, 1953; Godin, 1985, 1991, 1999; Jay, 1991; Horrevoets et al., 2004), and stimulating the generation of new harmonics (Proudman, 1953; Pingree and Maddock, 1978; Parker, 1984, 1991; Wang et al., 1999). Given all the three nonlinear terms are attributed to creating forced harmonics (Parker, 1984; Walters and Werner, 1991; Wang et al., 1999), it would be helpful to determine their relative importance. Gallo and Vinzon (2005) provided an evaluation of the relative importance of the nonlinear terms on overtide for the Amazon River estuary. But the results were only presented for a mean river discharge condition. It still remains an open question as to which nonlinear term plays a more significant role under varying river discharge conditions.

In this contribution we deploy a numerical model to explore river-tide interaction and subsequent impact on overtide behavior in a schematized long estuary. We aim to explore 1) how varying river discharge would modulate the overtides, and 2) what is the controlling impact of the nonlinear terms on the spatial variability of overtide under different river discharge.

2. Model setup and data analysis

2.1 Inspirations from the Changjiang River estuary

https://doi.org/10.5194/hess-2021-75
Preprint. Discussion started: 26 February 2021

The rationale of this study comes from tidal analysis in the Changjiang River estuary, which is a large tidal system with a tide-influenced river reach as along as 650 km (Figure 1a). River discharge at the tidal wave limit, Datong, varies seasonally in the range of 10,000-60,000 m^3/s in the post-Three Gorges Dam period (Figure 1b; Guo et al., 2018). The incoming tides are semi-diurnal with a maximum tidal range of 5.9 m, and the M_2 is the most significant constituent, followed by S_2, O_1, and K_1. Based on harmonic analysis (Pawlowicz et al., 2002) of tidal height data in the time periods when river discharge varies in a small range (close to a stationary situation, see Guo et al. (2016) for further details), we see that the incoming tidal waves are firstly amplified before they travel into the estuary, owing to a landward decrease in water depth (Figure 1c). They are, however, predominantly dissipated inside the estuary, despite the width convergence in the lower part of the estuary seaward of Jiangyin, because of stronger influence of bottom friction and/or river discharge. The river-enhanced tidal damping is more significant in the wet season when the river discharge is higher, particularly in the upper part of the estuary upstream of Jiangyin.

https://doi.org/10.5194/hess-2021-75
Preprint. Discussion started: 26 February 2021

Hydrology and Earth System Sciences
Discussions

137 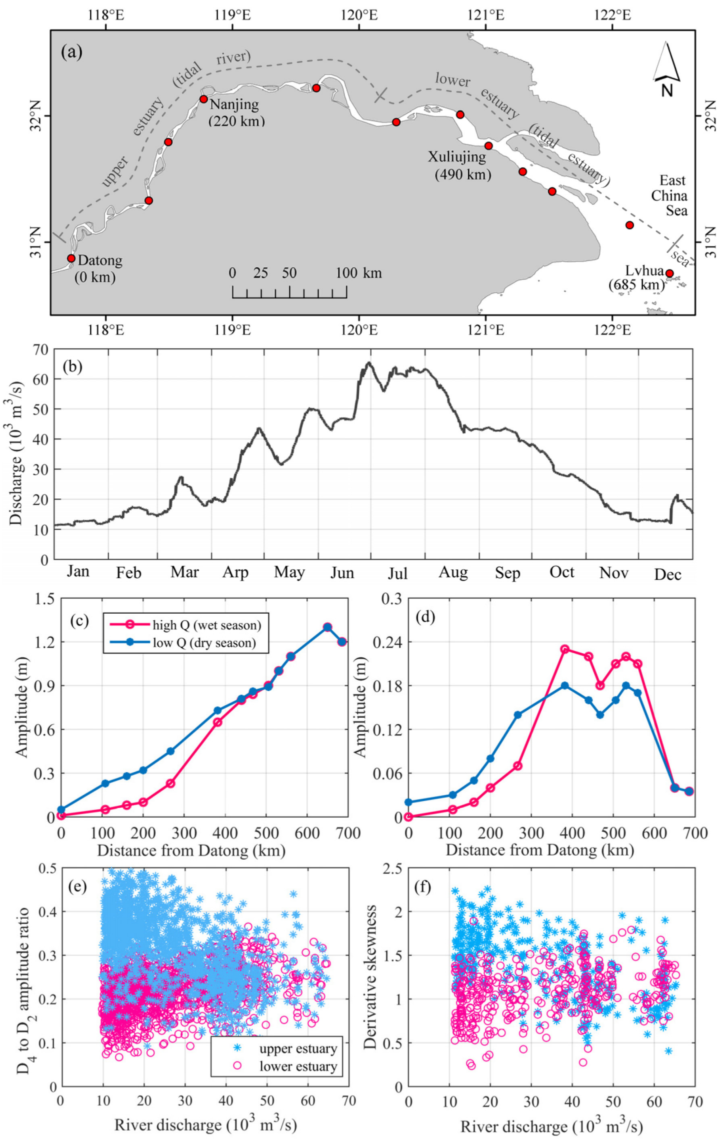

138 **Figure 1.** (a) The geometry and tidal gauges in the Changjiang River Estuary, 139 (b) river discharge variations within a year course, along-river (c) M_2, and (d) 140 M_4 amplitude variations in the dry and wet seasons, (e) amplitude ratios of the 141 quarter-diurnal to semi-diurnal tides, and (f) skewness of the time derivative of 142 tidal water levels in the upper (Nanjing) and lower (Xuliujing) estuaries. Details 143 of the Changjiang River estuary and the tidal data are given in Guo et al. 144 (2015). The numbers in the brackets in panel (a) indicate the seaward distance

https://doi.org/10.5194/hess-2021-75
Preprint. Discussion started: 26 February 2021

from Datong. The data in panels (c)-(e) is from Guo et al. (2016) and that in panel (f) is from Guo et al. (2019).

A significant M_4 overtide is detected inside the estuary while it is insignificant to seaward of the estuary (Figure 1d). The smaller M_4 amplitude in the region km-380 and km-520 in both dry and wet seasons is attributed to interaction between the two main branches around Xuliujing. Apart from that, the M_4 amplitude is larger in the lower part of the estuary in the wet season when the river discharge is higher (Figure 1d). Moreover, the amplitude ratios of the quarter- to semi-diurnal tidal species (derived by continuous wavelet transform) decrease with increasing river discharge in the upper part of the estuary but increase in the lower estuary (Figure 1e; Guo et al., 2015). Similar analyses, using the skewness of the time derivative of tidal water levels, show that the duration asymmetry between falling and rising tides exhibits similar variations as the amplitude ratios (Figure 1f; Guo et al., 2019). These results regarding the longitudinal M_4 amplitude variations by harmonic analysis (Figure 1d), the amplitude ratios of the quarter- to semi-diurnal tidal species (Figure 1e), and the derivative skewness variations (Figure 1f) consistently demonstrate that the overtides display distinctive variations between the upper and lower parts of the estuary in response to low and high river discharge conditions. However, such changing behavior was insufficiently discussed in previous studies. One challenge is that the river discharge varies continuously in reality and induces non-stationary variations in tidal dynamics. Conventional harmonic analysis is unable to accurately resolve the tidal changes when the river discharge varies continuously in a big range (Jay and Flinchem, 1997; Jay et al., 2014; Guo et al., 2015). Specifically, it is unknown how the overtides will behave as the river discharge varies between the low and high limits other than the results shown in Figure 1d.

2.2 Model setup

https://doi.org/10.5194/hess-2021-75
Preprint. Discussion started: 26 February 2021

Examination of tidal data has provided a basic framework for our understanding of tidal dynamics (Dronkers, 1964; Godin, 1985). However, conventional harmonic analysis may not accurately resolve tidal constituents owing to the non-stationary river discharge variations (Jay and Flinchem, 1997). In addition, analytical solutions of the tidal dynamic equations have facilitated exanimation of leading-order wave propagation such as landward damping or amplification of astronomical tides, given its advantages in terms of fast setup and transparency in unraveling physical processes (Jay, 1991; Friedrichs and Aubrey, 1994; Lanzoni and Seminara, 1998; Savenije, 2005). However, analytical models usually assume tidal propagation as a single wave component, based on simplified tidal dynamic equations after scaling analyses, e.g., adopting a linear assumption or a nonlinear expansion of the friction term (Green, 1837; Kreiss, 1957; Jay, 1991; Parker, 1991; Friedrichs and Aubrey, 1994; van Rijn, 2011). Analytical models may not fully capture the nonlinearity imbedded in tidal dynamics, considering that the importance of different nonlinear terms is likely not the same in different parts of long systems, particularly under strong river flow conditions in long estuaries.

In this study we seek to capture the nonlinear dynamics by using a numerical model, i.e., the open-source Delft3D codes, which has been widely validated and used in varying estuarine and coastal environments (Lesser et al., 2004). We construct a schematized 1D estuary model with a convergent planform mimicking the Changjiang River estuary. The model domain describes a 650 km long estuary that is composed of a weakly convergent upstream segment (km-0 to km-400, width varying from 2 to 5 km) and a strongly convergent downstream segment (km-400 to km-650, width varying from 5 to 32 km (Figure 2a). Another situation with a uniform prismatic channel (i.e., 2 km width and similar length) is adopted as part of the sensitivity analysis to see the influence of basin geometry (Figure 2b).

https://doi.org/10.5194/hess-2021-75
Preprint. Discussion started: 26 February 2021

Hydrology and Earth System Sciences
Open Access
Discussions

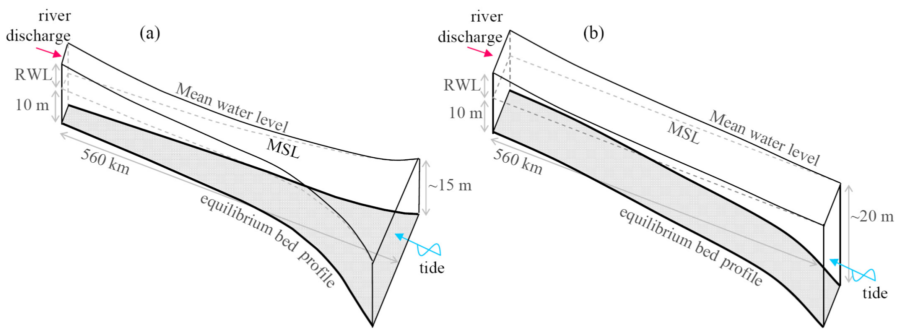

Figure 2. Sketches of the schematized estuary model outline and settings considering (a) a convergent and (b) a prismatic planform. The shade face indicates the equilibrium bed profile. The RWL and MSL indicate residual water level and mean sea level, respectively.

The model is forced by river discharge and tides. A combination of different tidal constituents is imposed, and for simplicity we mainly consider a semi-diurnal M_2 constituent with an amplitude of 1.0 m. Extra simulations considering both M_2 and S_2 constituents (an amplitude of 0.5 m) are included to facilitate more tidal interactions and generation of representative compound tide such as MS_4. Other astronomical constitutes like O_1 and K_1 are excluded because they would not affect the M_2 propagation very much. River discharge is prescribed by constant values of 0, 10,000, 30,000, 60,000 m^3/s, symbolized as Q0, Q1, Q3, and Q6 scenarios, respectively, to facilitate harmonic analysis with a stationary assumption. A dimensionless parameter, defined as the ratio of river discharge to tide-averaged mean discharge (i.e., tidal prism divided by tidal period) at the mouth section (R2T ratio), is estimated to be 0, 0.5, 2.6, and 42, which can be classified into tide-dominant, low, medium, and very high river discharge circumstances, respectively (see section 3.3). The size of the schematized estuary and the forcing conditions are characterized for a large river estuary and in this case key dimensions from the Changjiang River Estuary are used.

To obtain a suitable bottom profile for the tidal model, we first run a

https://doi.org/10.5194/hess-2021-75
Preprint. Discussion started: 26 February 2021

Hydrology and Earth System Sciences
Open Access
Discussions

morphodynamic simulation based on the above-mentioned model outline, with an M_2 tide and a river discharge seasonally varying between 10,000 and 60,000 m^3/s as the boundary forcing conditions, as that in Guo et al. (2016). The long-term morphodynamic simulation starts from an initial sloping bed with depth varying from 5 m to 15 m seaward, considers sediment transport and bed level changes, which leads to a morphodynamic equilibrium when bed level changes become small at the time scales greater than decades (Guo et al., 2016). The eventual equilibrium bed profile is then used as the bottom level condition in the tidal simulations. The purpose of using this equilibrium bed profile is to maintain consistency between the forcing and morphological conditions. Based on this equilibrium bed profile and given high river discharge imposed, the incoming tides are largely dissipated in the landward region of the estuary, thus the influence of wave reflection is minimized. Details of the morphodynamic model can be found in Guo et al. (2016), thus are not repeated here.

Past studies using similar 1D representation of tidal estuaries confirm the capture of leading-order dynamic processes (Friedrichs and Aubrey, 1994; Lanzoni and Seminara, 1998). But it is noteworthy that the 1D model excludes tidal flats and assumes uniform water density. These excluded processes may have additional impact on tidal dynamics, e.g., additional momentum loss, reduction in bottom drag, and extra tidal asymmetry (Friedrichs and Aubrey, 1988; Talke and Jay, 2020). Although simplified, the model provides a virtual lab where tidal wave propagation, deformation and associated overtide dynamics under varying river discharge can be isolated from the influences of basin geometry and irregular shoreline, which enables straightforward exploration of river-tide interactions.

2.3 Data analysis

The 1D model solves the width-averaged shallow water equations, i.e., the continuity and momentum conservation equations, when the effect of Coriolis

https://doi.org/10.5194/hess-2021-75
Preprint. Discussion started: 26 February 2021

force and density variations are neglected (Dronkers, 1964), as follows,

$$\frac{\partial \eta}{\partial t}+\frac{\partial u(h+\eta)}{\partial x}=0 \tag{1}$$

$$\frac{\partial u}{\partial t}+u\frac{\partial u}{\partial x}+g\frac{\partial \eta}{\partial x}+\frac{gu|u|}{C^2(h+\eta)}=0 \tag{2}$$

where u is velocity, η is water height above mean sea level, h is water depth below mean sea level, g is gravitational acceleration (9.8 m^2/s), and C is a Cheźy friction coefficient prescribed as 65 m$^{1/2}$/s uniformly.

As the bed level is prescribed as an equilibrium profile, the water depth h is constant. In the presence of a river discharge, the water level height is composed of two parts, namely a mean water height related to river flow η_0, and a tide-induced water level oscillation,

$$\eta(x,t)=\eta_0(x)+\eta_{M2}(x)\cos(\omega t-kx) \tag{3}$$

in case of the presence of M_2 tide only, in which η_{M2} is the surface amplitude of M_2, and ω is the frequency of M_2, and k is tidal wave number. Similarly, the current is composed of a mean current and a tidal component,

$$u(x,t)=u_0(x)+u_{M2}(x)\cos(\omega t-kx-\theta) \tag{4}$$

in which u_0 is the mean current velocity, u_{M2} is the velocity amplitude of M_2, θ is the phase difference between tidal surface wave and tidal currents.

Three nonlinear terms are identified in the tidal wave equations, namely the discharge gradient term in the continuity equation, and the advection and quadratic friction terms in the momentum equation:

- discharge gradient: $\frac{\partial u(h+\eta)}{\partial x}=\frac{\partial (uh)}{\partial x}+\frac{\partial (u\eta)}{\partial x}$ (5)
- advection: $u\frac{\partial u}{\partial x}=\frac{\partial}{\partial x}(\frac{u^2}{2})$ (6)
- bottom friction: $\frac{gu|u|}{C^2(h+\eta)}\approx\frac{g}{C^2}(\frac{u|u|}{h}-\frac{\eta u|u|}{h^2})$ (7)

The bottom friction term is approximately expanded into a bottom shear stress term and a term considering depth variations, as the two terms on the right hand of Eq. (7), respectively, according to Godin and Martinez (1994), given the tidal amplitude to water depth ratio ($|\eta|/h$) is generally smaller than

https://doi.org/10.5194/hess-2021-75
Preprint. Discussion started: 26 February 2021

Hydrology and Earth System Sciences
Open Access
Discussions

one. Note that the bottom friction term can be calculated accurately with resolved water depths and velocities in the numerical model, while the approximation of Eq. (7) is just used to analytically demonstrate how the friction would lead to local generation of compound tides and overtides. Firstly considering a situation when river discharge is small and the associated mean current (u_0) is insignificant, the quadratic bottom stress can be further expressed by Fourier decomposition according to Le Provost (1991) and Wang et al. (1999):

$$\frac{u|u|}{h} \approx \frac{u_{\mathrm{M2}}^2}{h} \sum_{n=0,1,2,...} (-1)^{n+1} \frac{8}{(2n-1)(2n+1)(2n+3)\pi} \cos(2n+1)\omega t \cos(nkx) \qquad (8)$$

Equation (8) suggests that the self-interaction of M_2 tide through the quadratic bottom stress produces a series of overtide harmonics with odd-multiple frequencies, e.g., M_6 and M_{10} (Parker, 1984). In addition, Eq. 8 also yields a contribution to the same frequency as M_2 (when n=0), which suggests tidal energy dissipation via the quadratic shear stress term (Wang et al., 1999). Similarly, the depth variation term in Eq. 7 can be expressed as:

$$\frac{\eta u|u|}{h^2} \approx \frac{\eta_{M2} u_{\mathrm{M2}}^2}{h^2} \sum_{n=0,1,2,...} (...) \ \cos(\omega t)\cos[(2n+1)\omega t]$$

$$= \frac{\eta_{M2} u_{\mathrm{M2}}^2}{h^2} \sum_{n=0,1,2,...} (...) \ [\frac{1}{2}\cos(2n\omega t) + \frac{1}{2}\cos(2n+2)\omega t] \qquad (9)$$

Equation (9) suggests that the self-interaction of M_2 tide through the depth variation term generates even-multiple frequency harmonics, e.g., M_4 and M_8. Similar decomposition analysis for the advection and discharge gradient term suggests the generation of even-frequency overtide as well (Parker, 1984; Wang et al., 1999). Following similar logic, when two components such as M_2 and S_2 tides are prescribed, compound tides with frequencies the sums (e.g., MS_4) or differences (e.g., MSf) of the prescribed constituents are generated. The main focus of this study is devoted to M_4 overtide, given it is the first overtide of M_2 and of profound importance for tidal asymmetry.

Following the above analyses that qualitatively indicates the possibility of

https://doi.org/10.5194/hess-2021-75
Preprint. Discussion started: 26 February 2021

Hydrology and Earth System Sciences
Discussions

local overtide generation, we attempt to further quantify the relative contribution of the nonlinear terms. For this purpose, we employ another approximation of the quadratic shear stress term, as follows, according to Godin and Martinez (1994) and Godin (1999),

$$u|u| \approx 0.35u + 0.71u^3 \tag{10}$$

Replacing the Eq. (7) with Eq. (10) and using the expansion of Eqs. (3) and (4), a harmonic decomposition using the sine and cosine summation rules is used to identify the contribution of the nonlinear discharge gradient, advection, and bottom friction terms based on Eqs. (5) to (7). It follows the method in Gallo and Vinzon (2005) and Leberthal et al. (2019), but considering both quadratic bed shear and depth variation terms.

- discharge gradient: $0.5u_{M2}\frac{\mathrm{d}\eta_{M2}}{\mathrm{d}x} + 0.5\eta_{M2}\frac{\mathrm{d}u_{M2}}{\mathrm{d}x}$ (11)
- advection: $0.5u_{M2}\frac{\mathrm{d}u_{M2}}{\mathrm{d}x}$ (12)
- friction: $\frac{1.065g}{C^2h}u_0u_{M2}^2 + \frac{g}{C^2h^2}[1.065\eta_0u_0u_{M2}^2 + 0.525u_0^2\eta_{M2}u_{M2} + 0.355\eta_{M2}u_{M2}^3]$ (13)

The first term in Eq. 13 is ascribed to the quadratic bottom shear while the other terms are attributed to the depth variations. Again, the Eqs. (11) to (13) suggest that the interaction between the mean current and M_2 velocity would generate even-frequency harmonics like M_4 via both the quadratic bed shear stress and depth variation terms, implying river influence through river-tide interaction. Harmonic analyses of the model-output time series of water levels and currents provide mean water height, mean current, and the amplitudes and phases of surface wave and velocity of M_2 and M_4 tides for Eqs. (11) to (13). To indicate their relative importance, the advection and friction terms are then normalized by squared maximum velocity, and the discharge gradient term is normalized by the product of maximum velocity and maximum water level range. Comparison of the four scenarios forced by different river discharge thus helps to demonstrate the variability (see section 3.3).

https://doi.org/10.5194/hess-2021-75
Preprint. Discussion started: 26 February 2021

3. Model results

3.1 Tidal variations under varying river discharge

The longitudinal amplitude variations of both the principal and forced constituents are shown in Figure 3. The M_2 tide is firstly slightly amplified in the utmost seaward regions close to the mouth, owing to channel convergence, (Figure 3a). Landward of that, the incoming M_2 tide is predominantly dissipated, and river discharge enhances the damping. In addition, a considerable M_4 tide is detected in the Q0 scenario (no river discharge) with a local amplitude maximum around km-450. The M_4 amplitude becomes larger throughout the estuary in the Q1 scenario compared with that that in Q0 (Figure 3b). However, under higher river discharge, the M_4 amplitude reduces in the upper part of the estuary, e.g., landward km-300, but continues to increase in the lower reaches, e.g., seaward km-500 (Figure 3b). The location with maximal M_4 amplitude moves slightly landward as the river discharge increases from zero (i.e., from km-450 in the Q0 scenario to km-400 in the Q1 scenario), but seaward as the river discharge further increases (i.e., from km-420 in the Q3 scenario to km-500 in the Q6 scenario). The M_4 to M_2 amplitude ratio exhibits similar variations as the absolute M_4 amplitude, but the ratio is overall larger in the upper parts of the estuary in which the absolute amplitudes of both M_2 and M_4 tides are small (Figure 3d). The increasingly damped and distorted tidal waves further illustrate the river impact on the incoming tides (see Figure S1 in the SI). When both M_2 and S_2 are imposed in the seaward boundary, a compound overtide MS_4 is detected inside the estuary, which exhibits similar spatial variations as the M_4 tide (Figure 3c). We then focus on the M_4 overtide in the following discussions.

https://doi.org/10.5194/hess-2021-75
Preprint. Discussion started: 26 February 2021

Hydrology and Earth System Sciences
Discussions

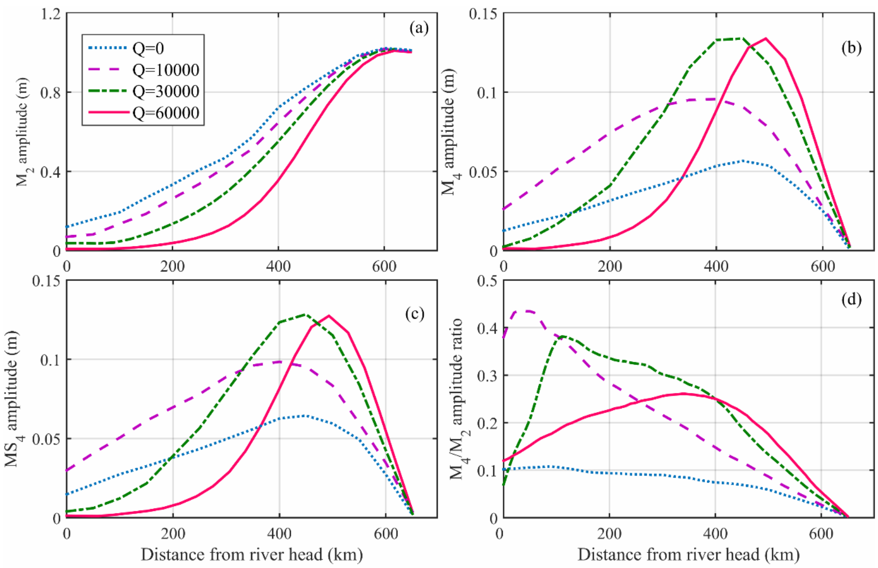

Figure 3. The model-reproduced longitudinal variations of (a) M_2 tidal amplitude, (b) M_4 tidal amplitude, (c) MS_4 amplitude (in the extra scenario when both M_2 and S_2 are imposed at the boundary), and (d) the M_4 to M_2 amplitude ratios in the convergent estuary.

3.2 Sensitivity to channel convergence

Channel convergence is expected to affect tidal wave propagation and wave deformation (Jay, 1991; van Rijn, 2011; Talke and Jay, 2020). To demonstrate the sensitivity of the model results to width variations, we setup a prismatic channel model with similar settings as the convergent estuary. A close-to-equilibrium bed profile is again obtained via morphodynamic simulation for the prismatic estuary. River discharge elevates the mean water level and mean current (Figure 4a). The incoming M_2 tide is overall damped inside the estuary, without any amplification (Figure 4b). Similar M_4 overtide is generated as well, but its amplitude is approximately 30% smaller than that in the convergent estuary (Figure 4c). A smaller tidal prism owing to a smaller mouth width and surface area explain the smaller tidal amplitude in the rectangular estuary. Apart from the differences in the absolute amplitudes, the

https://doi.org/10.5194/hess-2021-75
Preprint. Discussion started: 26 February 2021

longitudinal variations of both the principal and forced tides and their spatial dependence on river discharge exhibit similar patterns as the convergent estuary (Figures 3 and 4). These consistent results imply that channel convergence does not fundamentally changes the spatial dependence of overtide behavior on river discharge, thus the findings from the prismatic estuary is taken to have implications for estuaries in general and will be the focus of further more detailed examination in order to highlight the controlling impact of river discharge.

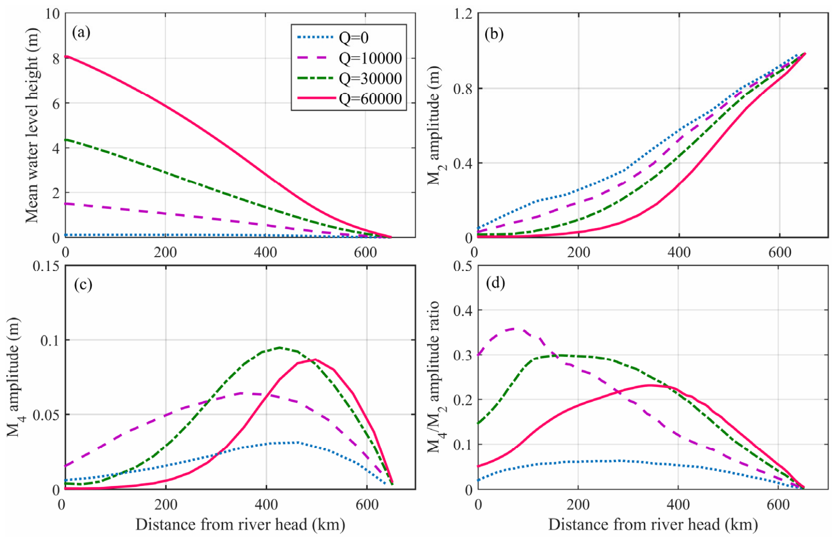

Figure 4. Model-reproduced longitudinal variations of (a) mean water level height, (b) M_2 tidal amplitude, (d) M_4 tidal amplitude, and (d) the M_4 to M_2 amplitude ratio under different river discharge in the prismatic estuary.

3.3 Contribution of the nonlinear terms

We then use the harmonic decomposition method proposed in section 2.3 to quantify the contribution of the different nonlinear terms on M_4 variations. In the absence of river discharge (Q0 scenario), the discharge gradient term is the largest contribution owing to strong landward damping of M_2 and subsequent longitudinal flux gradients, followed by bottom friction and advection (Figure 5a). The bottom friction term becomes more significant in the

https://doi.org/10.5194/hess-2021-75
Preprint. Discussion started: 26 February 2021

presence of river discharge (Figures 5b-d). The impact of the quadratic bottom shear stress is much more important than that of depth variations. The influence of the advection term is relatively small compared to the other two nonlinear terms. Spatially, the impact of bottom friction is more profound in the upper parts of the estuary, whereas the impact of discharge gradient and advection is more apparent in the regions close the estuary mouth. The location of maximal M_4 amplitude coincides with the peak in the combined contribution of discharge gradient and advection in the Q0 scenario, but with the peak in bottom friction in the other three scenarios. Overall, these results suggest that the three nonlinear terms are equally important in the tide-dominated long estuary, whereas the importance of the bottom friction, or more precisely the quadratic bottom shear stress, stand out when there is significant river discharge.

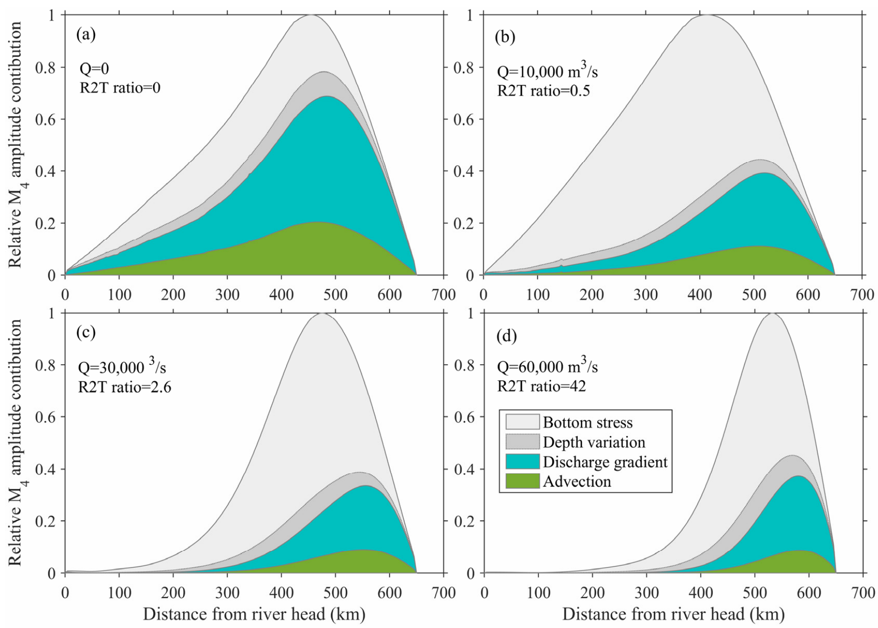

Figure 5. Quantification of the relative importance of three nonlinear terms on M_4 overtide amplitude in the (a) Q=0 (R2T ratio=0), (b) Q=10,000 (R2T ratio=0.5), (c) Q=30,000 (R2T ratio=2.6), and (d) Q=60,000 m^3/s (R2T ratio=42) scenarios. The contribution of bottom friction is divided into the components of

https://doi.org/10.5194/hess-2021-75
Preprint. Discussion started: 26 February 2021

bottom shear stress and depth variation. The relative M_4 amplitude is normalized by the maximal value in each scenario.

The importance of the quadratic bottom shear stress can be furthermore inferred when comparing the model results under quadratic and linear bottom shear stress. The quadratic bottom shear stress can be linearized using the first order of the energy dissipation condition (Lorentz, 1926), as that applied by Zimmerman (1992) and Hibma et al. (2003) (see SI for more details). When similar simulations are run using linear bottom stress, the landward damping rates of the principal tides become smaller (see Figure S4). Measurable M_4 overtide is still detected, which is ascribed to the effects of other nonlinear effects (e.g., the advection and depth variations), but its amplitude is comparably smaller than that under a quadratic bottom stress (Figure S4). Moreover, increasing river discharge neither induces more tidal wave damping, nor more overtide generation under a linear bottom stress.

3.4 Quantification of the river discharge threshold

The abovementioned model results imply that the M_4 amplitude tends to first increase and then decrease as the principle M_2 is increasingly dissipated by larger river discharge. To better reveal the nonlinear variations, we run extra simulations under constant river discharge in the range of 0 to 60,000 m^3/s at an increment of 5,000 m^3/s. Since the tidal amplitudes vary along the estuary, we then integrate the total (tide-averaged) energy of M_2 and M_4 tides ($kg \cdot m^2/s^2$) throughout the estuary to represent overall tidal strength (van Rijn, 2011) by：

$$\int_0^L 0.5 \rho g b A(x)^2 dx / L \tag{14}$$

where: L is the channel length, ρ is the water density, b is channel width which is uniform in the rectangular channel, and A is the surface amplitude of the M_2 or M_4 tide which varies along the estuary.

We see that the total energy of the M_2 tide decreases approximately

https://doi.org/10.5194/hess-2021-75
Preprint. Discussion started: 26 February 2021

Hydrology and Earth System Sciences
Discussions
Open Access

exponentially with increasing R2T ratios (Figure 6a). The decrease is more significant for R2T<5 (see Figure S2a). The total energy of M_4 overtide, however, first increases with increasing R2T ratio from zero and reaches a peak when the R2T ratio is approximately unity, followed by a decrease as the R2T ratio further increases (Figure 6a). The maximum total energy of M_4 is 4.7 times the case with no river discharge, under the model framework in this study. Similarly, the energy ratio of M_4 to M_2 displays similar variations as the total energy variation of the M_4 tide, with a peak reached when the R2T ratio is around 1-2 (Figure 6b). These results confirm that an intermediate river discharge with R2T ratio close to unity, benefits maximal M_4 overtide generation. Below this threshold, increased river discharge favors more M_4 tide generation, whereas a larger river discharge above the threshold constrains M_4 generation.

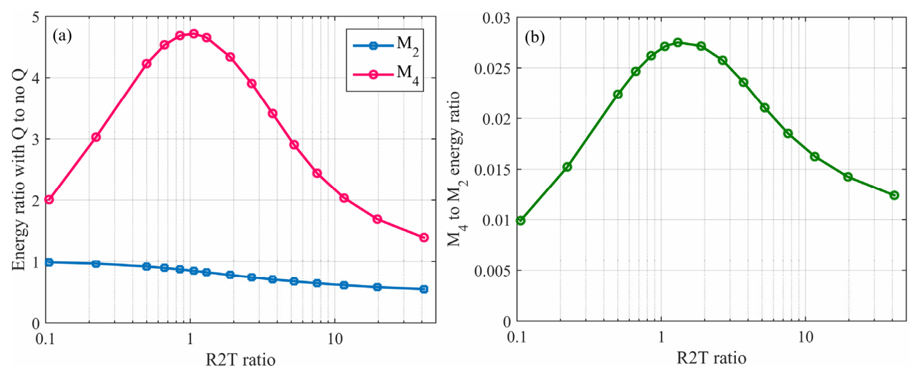

Figure 6. (a) The ratio of the total energy of M_2 and M_4 tides integrated throughout estuary in the scenarios with river discharge to the case without river discharge, and (b) the total energy ratio of M_4 tide to M_2 tide, as a function of the ratio of river discharge to tide-mean discharge at the estuary mouth (R2T ratio). Also see Figure S2 in the SI.

4. Discussion

4.1 Comparison with actual estuaries

The findings regarding overtide variability in the model are overall

https://doi.org/10.5194/hess-2021-75
Preprint. Discussion started: 26 February 2021

consistent with data analyses in actual estuaries like the Changjiang and Amazon River estuaries. The modeled results between the Q1 and Q3 scenarios are consistent with the along-channel variations of the principle tide and overtide under low and high river discharge in the Changjiang River Estuary. The changes in the M_4 to M_2 amplitude ratios with varying river discharge between the upper and lower parts of the Changjiang River Estuary also agree well with model results in the schematized convergent estuary (see Figure S3). In the Amazon River estuary where the river discharge is similarly high and varies in a large range, the M_4 amplitude was overall larger under a mean river discharge throughout the estuary compared to an idealized situation with zero discharge (Figure 7c; Gallo and Vinzon, 2005). This result is qualitatively consistent with the modeled differences between the Q0 and Q1 scenarios in this study. In the Columbia River estuary, a maximum in M_4 amplitude is approached in the lower part of the estuary, followed by a subsequent decrease upriver under a year-mean river discharge (Figure 7d; Jay et al., 2014). The model results can also explain why a higher river discharge hastened the high water and delayed the low water in the lower part of the Saint Lawrence Estuary (Godin, 1985, 1999). These field data and model results confirm that the findings regarding the spatial dependence of overtide on river discharge are likely to be ubiquitous for river estuaries.

Similar reports of the overtide behavior were, however, not widely found in many other estuaries, given that the tidal dynamics have been intensively studied worldwidely. We think that it maybe because the majority of estuaries worldwide are tide-dominated, such that river discharge is overall small and rarely reaches a magnitude that exceeds R2T=1. Therefore, the role of river discharge in stimulating wave deformation and associated overtide generation has been widely observed and confirmed (when R2T<1), whereas the further changes when R2T>1 are far less prevalent and hence less well documented. Another possible explanation is that most tidal estuaries are small in physical length (compared to wavelength), hence the spatial variations are less

https://doi.org/10.5194/hess-2021-75
Preprint. Discussion started: 26 February 2021

apparent compared to long estuaries such as the Amazon, Changjiang, and Columbia systems.

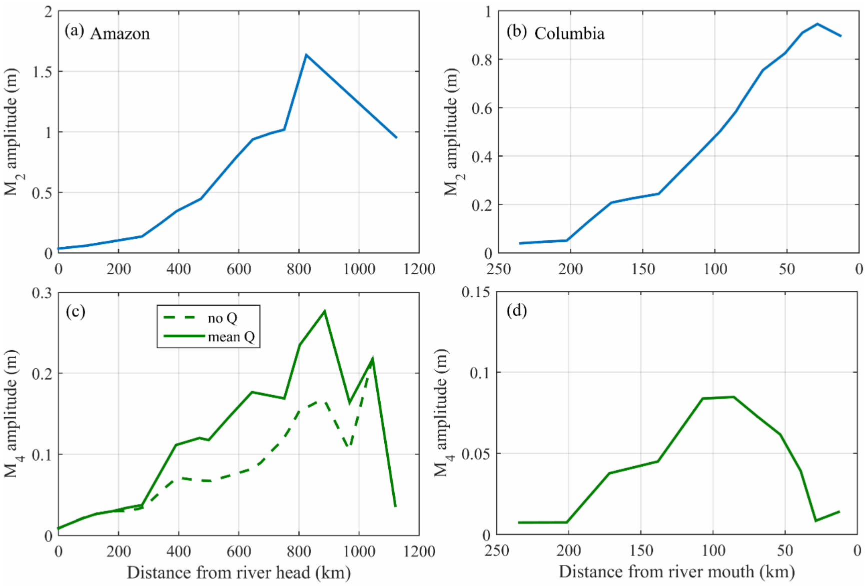

Figure 7. Amplitude variations of M2 and M4 overtide in the (a, c) Amazon River estuary and (b, d) Columbia River estuary, from Gallo and Vinzon (2005) and Jay et al. (2014), respectively.

4.2 Role of river discharge

The majority of past studies have focused on either the damping effect of river flow on principal tides or the enhancing effect on overtide. When linking them together, we see that the two-fold effects of river flow nicely explain the nonlinear overtide changes in river estuaries (Figure 8). River discharge enlarges the currents and the effective friction on the moving flow. It induces more damping of the principal tides, i.e., more energy dissipation of incident tides. In addition, river-enhanced bottom friction reinforces the energy transfer from the principal tide to overtide, i.e., stimulated overtide generation. As more principal tidal energy is dissipated, particularly in the landward part of estuaries, the energy available for transfer to overtide is also constrained. As a result, an intermediate river discharge (when the R2T ratio is close to unity) provides an effective bottom stress that will not dissipate the principal tides too much, and at the same time stimulates considerable energy transfer to overtides, leading to the occurrence of a maximum in overtide energy. Note that other high-frequency overtides display similar spatial variations as M_4, e.g., MS_4 (see Figure 3c) and MN_4 tide when M_2 and N_2 constituents are prescribed (not shown).

River impact on tidal wave propagation is space-dependent. River discharge substantially elevates the mean water level in the upper part of estuaries; the consequent larger water level gradient restricts landward wave propagation (Godin, 1985; Cai et al., 2019). In the lower part of estuaries where the incident tides are less dissipated, river flow plays a more important role in reinforcing the effective bottom friction. As a result, dissipation of the principal tide is more prominent in the upper part of estuaries, while tidal energy transfer and overtide generation is more substantial in the lower part of estuaries (Figures 8). These space-dependent dynamics explain the contrasting behavior of overtide in response to increasing river discharge, and also confirm that tidal wave deformation maybe one of the degrees-of-freedom of estuaries to maintain a state of minimum work by adjusting tidal wave shapes in response to different river discharge (Zhang et al., 2016).

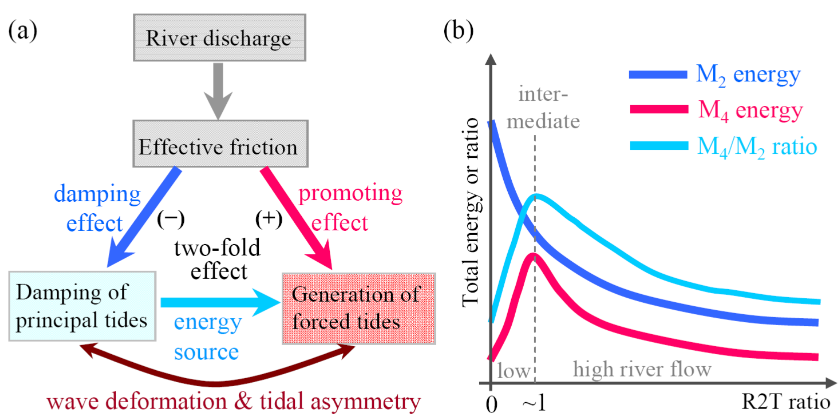

Figure 8. Sketches (a) showing the two-fold effects of river discharge on tides mainly through the bottom friction, and (b) showing the intermediate river

discharge threshold that benefits maximum overtide generation.

The two-fold river impact on tidal propagation is coherently related to the bottom friction. Past studies have indicated that the effects of river flow on tidal damping are exerted by a mechanism identical to bottom stress (Horrevoets et al., 2004; Cai et al., 2014). River-tide interaction enhances the bottom stress, which subsequently induces larger tidal damping (Alebregtse and de Swart, 2016). Past studies have also suggested that the nonlinear advection term is the main cause of M_4 generation in tide-dominant estuaries, whilst the nonlinear bottom stress term leads to generation of M_6 (Pingree and Maddock, 1978; Parker, 1984, 1991; Wang et al., 1999). In this work we see that the quadratic bottom stress term also leads to significant M_4, through river-tide interaction, i.e., between a river-enhanced mean current and M_2 current. This explains why the M_4 amplitude is larger in the presence of a river discharge and a quadratic bottom stress, compared to the situation with no river discharge and/or a linear bottom stress.

Given the comprehensive past studies of tidal dynamics in estuaries, the contribution of this work lies in revealing the nonlinear overtide changes and identification of a river discharge threshold that benefit maximum overtide generation. A river flow above or below the threshold induce contrasting overtide behavior along estuaries. Although the model results are obtained under constant river discharge, the findings still hold true when considering time-varying river discharge (see SI). One slight difference is that the tidal damping rate would be slightly different during the rising and falling limb of a river discharge hydrograph (Sassi and Hoitink, 2013), which may be due to a time lag in the influence of river discharge along the length of the estuary.

4.3 Implications and limitations

Better understanding of the overtide behavior has implication for studies of tidal bores, interpretation of extreme high water and associated flood risk, and

https://doi.org/10.5194/hess-2021-75
Preprint. Discussion started: 26 February 2021

Hydrology and Earth System Sciences
Discussions
Open Access

tide-averaged sediment transport. Tidal wave deformation changes the height of high water and low water, which may then influence flooding risk management and the water depth of navigational channels. Tidal bores are an extreme phenomenon of tidal wave deformation when tides are concurrently amplified and distorted to some degree (Bonneton et al., 2015). Tidal bores are less likely to occur in river estuaries because of river-enhanced damping, although deformation is enhanced. The interaction between tidally-averaged mean current and quarter-diurnal overtide current may contribute to net water transport (Alebregtse and de Swart, 2016). Tide-averaged sediment transport induced by tidal asymmetry related to M_2-M_4 interaction plays a profound role in controlling sediment import or export and resultant infilling or empty of estuaries (Postma, 1961; Guo et al., 2014). It is noteworthy that the horizontal velocity of the quarter-diurnal tide may exhibit more spatial variations than its surface amplitude, owing to interaction with estuarine morphology and inter-tidal interactions of eddy viscosity etc. (Dijkstra et al., 2017b; Lieberthal et al., 2019).

Although we have argued that channel convergence will not fundamentally change the model results and main findings, the potential impact of the simplified model setting in this study still mandates careful evaluation when applying them to actual estuaries. For instance, regional narrowing and shallowness in geometry and morphology is expected to induce variations in tidal damping rates and distribution of amplitudes. River-influenced estuaries can be partially or highly stratified, and a density difference and associated stratification affect tides by reducing the effective drag coefficient and changing the pressure-gradient term (Talke and Jay, 2020). This impact maybe further manifested in surface amplitude of overtide given the role of river-tide current interaction in the nonlinear terms (Dijkstra et al. 2017a). Inter-tidal flats are known as a sink of momentum and would exert additional impact on tidal wave propagation (Hepkema et al., 2018). Exclusion of inter-tidal flats in this work thus may lead to overestimation of the overtide amplitude. Furthermore, the

https://doi.org/10.5194/hess-2021-75
Preprint. Discussion started: 26 February 2021

intermediate river discharge threshold that satisfies R2T=1 is expected to vary with estuarine size and shape, given that the tidal mean discharge is strongly affected by estuarine morphology. These dynamic complexities merit further study for site-specific cases.

5. Conclusions

Based on past intensive studies of tidal dynamics in estuaries, this work is devoted to examining the forced overtide behavior under varying river discharge and the controlling nonlinear mechanism. We use a numerical model for a schematized long estuary to capture the nonlinear dynamics as much as possible. Model results reveal local overtide generation whose amplitude however exhibits strong spatial dependence. While the principal M_2 tide is increasingly dissipated as the R2T ratio increases from zero, the M_4 overtide amplitude decreases in the upper part of estuaries but increases in the lower part of estuaries. With increasing R2T ratio, the total energy of M_4 overtide integrated throughout the estuary first increases and reaches a peak when the R2T ratio approaches unit. Further larger river discharge induces a decline in total energy of both M_2 and M_4. The modeled nonlinear changes in overtide are quantitatively validated by data in actual estuaries like the Changjiang and Amazon River estuaries.

Further sensitivity simulations confirm the significant role of bottom friction that is enhanced by river-tide interaction in controlling the overtide behavior. The effective bottom friction is enhanced by the river discharge, and this has two-fold impact: (1) dissipation of principal tidal energy and (2) stimulation of energy transfer to overtides. The two-fold effect explains the occurrence of an intermediate river discharge threshold that benefits maximal overtide amplitude. This study demonstrates the need to look at both tidal wave propagation and deformation at the same time in tidal wave dynamics, as well as their nonlinear spatial variations in large river estuaries. The findings have implications for study of tidal bores and tidal asymmetry and associated morphological changes in river estuaries.

Author contribution

LG designed the experiments and carried them out. LG and IT prepared the manuscript with contributions from all co-authors.

Declare of interest conflict

The authors declare that they have no conflict of interest.

Data availability

The model data are available on request at the corresponding author.

Acknowledgements

This work is supported by the project 'Coping with deltas in transition' within the Programme of Strategic Scientific Alliance between China and The Netherlands (PSA), financed by the Ministry of Science and Technology, P.R. China (MOST) (No. 2016YFE0133700) and Royal Netherlands Academy of Arts and Sciences (KNAW) (No. PSA-SA-E-02), and also partly by MOST (No. 2017YFE0107400), National Natural Science Foundation of China (Nos. 51739005; U2040216; 41876091), Shanghai Committee of Science and Technology (Nos. 19QA1402900; 20DZ1204700), and the Fundamental Research Funds for the Central Universities. We thank David A. Jay (PSU, USA) and Henk M. Schuttelaars (TU Delft, the Netherlands) for their comments and suggestions.

References

Alebregtse N.C., de Swart H.E., 2016. Effect of river discharge and geometry on tides and net water transport in an estuarine network, an idealized model applied to the Yangtze Estuary. Continental Shelf Research 123, 29-49.

Bonneton P., Bonneton N., Parisot J.-P., Castelle B., 2015. Tidal bore dynamics in funnel-shaped estuaries. Journal of Geophysical Research: Oceans 120, 923-941.

Buschman F.A., Hoitink A.J.F., van der Vegt M., Hoekstra P., 2009. Subtidal water level variation controlled by river flow and tides. Water Resources Research 45, W10420, doi:10.1029/2009WR008167.

Cai H.Y., Savenije H.H.G., Toffolon M., 2014. Linking the river to the estuary: influence of river discharge on tidal damping. Hydrology and Earth System Science 18, 287–304.

Cai H.Y., Savenije H.H.G., Garel E., Zhang X.Y., Guo L.C., Zhang M., Liu F.., Yang Q.S., 2019. Seasonal behaviors of tidal damping and residual water level slope in the Yangtze River estuary: identifying the critical position and river discharge for maximum tidal damping. Hydrology Earth System Science 23, 2779–2794.

Dijkstra Y.M., Brouwer R.L., Schuttelaars H.M., Schramkowski G.P., 2017a. The iFlow modelling framework v2.4: a modular idealized process-based model for flow and transport in estuaries. Geoscientific Model Development 10, 2691-2731.

Dijkstra Y.M., Schuttelaars H.M., Burchard H., 2017b. Generation of exchange flows in estuaries by tidal and gravitational eddy viscosity-shear covariance (ESCO). Journal of Geophysical Research: Oceans 122, 4217-4237.

Dronkers J.J., 1964. Tidal computations in rivers and coastal waters. North-Holland, Amsterdam, pp.219–304.

Friedrichs C.T., Aubrey D.G., 1988. Non-linear tidal distortion in shallow well-mixed estuaries: a synthesis. Estuarine, Coastal and Shelf Science 27, 521-545.

Friedrichs C.T., Aubrey D.G., 1994. Tidal propagation in strongly convergent channels. Journal of Geophysical Research 99, 3321–3336.

Gallo M.N., Vinzon S.B., 2005. Generation of overtides and compound tides in the Amazon Estuary. Ocean Dynamics 55, 441-448.

Godin G., 1985. Modification of river tides by the discharge. Journal of

Waterway, Port, Coastal and Ocean Engineering 111(2), 257–274.

Godin G. 1991. Frictional effects in river tides. In: B.B. Parker (ed.), Tidal hydrodynamics, John Wiley, Toronto, pp.379–402.

Godin G., 1999, The propagation of tides up rivers with special consideration of the upper Saint Lawrence River. Estuarine, Coastal and Shelf Science, 48, 307–324.

Godin G., Martinez A., 1994. Numerical experiment to investigate the effect of quadratic friction on the propagation of tides in a channel. Continental Shelf Research 14, 723-748.

Guo L.C., Su N., Zhu C.Y., He Q., 2018. How have the river discharges and sediment loads changed in the Changjiang River basin downstream of the Three Gorges Dam? Journal of Hydrology 560, 259-274.

Guo L.C., van der Wegen M., Jay D.A., Matte P., Wang Z.B., Roelvink J.A., He Q., 2015. River-tide dynamics: exploration of nonstationary and nonlinear tidal behavior in the Yangtze River estuary. Journal of Geophysical Research: Oceans 120, doi:10.1002/2014JC010491.

Guo L.C., van der Wegen M., Wang Z.B., Roelvink J.A., He Q., 2016. Exploring the impacts of multiple tidal constituents and varying river flow on long-term, large scale estuarine morphodynamics by means of a 1D model. Journal of Geophysical Research: Earth Surface 120, doi:10.1002/2016JF003821.

Guo L.C., Wang Z.B., Townend I., He Q., 2019. Quantification of tidal asymmetry in varying tidal environments. Journal of Geophysical Research: Oceans 124, 773-787.

Hepkema T.M., de Swart H.E., Zagaris A., Duran-Matute M., 2018. Sensitivity of tidal characteristics in double inlet systems to momentum dissipation on tidal flats: a perturbation analysis. Ocean Dynamics 68, 439-455.

Hibma A., H.M. Schuttelaars, Z.B. Wang. 2003. Comparison of longitudinal equilibrium profiles of estuaries in idealized and process-based models. Ocean dynamics, 53, 252–269.

https://doi.org/10.5194/hess-2021-75
Preprint. Discussion started: 26 February 2021

Hoitink A.J.F., Jay D.A., 2016. Tidal river dynamics: implications for deltas. Reviews of Geophysics 54, 240–272.

Horrevoets A.C., Savenije H.H.G., Schuurman J.N., Graas S., 2004. The influence of river discharge on tidal damping in alluvial estuaries. Journal of Hydrology, 294, 213–228.

Jay D.A., 1991. Green's law revisited: tidal long-wave propagation in channels with strong topography, Journal of Geophysical Research 96, 20585–20598.

Jay D.A., Leffler K., Diefenderfer H.L., Borde A.B., 2014. Tidal-fluvial and estuarine processes in the lower Columbia River: I. along-channel water level variations, Pacific Ocean to Bonneville Dam. Estuaries and Coasts, doi: 10.1007/s12237-014-9819-0.

Kästner K., Hoitink A.J.F., Torfs P.J.J.F.,, Deleersnijder E., Ningsih N.S., 2019. Propgation of tides along a river with a sloping bed. Journal of Fluid Mechanics 872, 39-73.

Kreiss H., 1957. Some remarks about nonlinear oscillations in tidal channels. Tellus 9, 53–68.

Le Provost C., 1991. Generation of overtides and compound tides (review). In: B.B. Parker (ed.), Tidal Hydrodynamics, John Wiley, Toronto, pp.269–295.

Lieberthal B., Huguenard K., Ross L., Bears K., 2019. The generation of overtides in flow around a headland in a low inflow estuary. Journal of Geophysical Research: Oceans 124, 955-980.

Lu S., Tong C.F., Lee D.-Y., Zheng J.H., Shen J., Zhang W., Yan Y.X., 2015. Propagation of tidal waves up in the Yangtze Estuary during the dry season. Journal of Geophysical Research: Oceans 120, 6445-6473.

Matte P., Jay D.A., Zaron E.D., 2013. Adaptation of classical tidal harmonic analysis to nonstationary tides, with application to river tides. Journal of Atmosphere and Oceanic Technology 30(3), 569-589.

Parker B.B., 1984. Frictional effects on tidal dynamics of shallow estuary. PhD. Dissertation, The Johns Hopkins University, 291 pp.

Parker B.B., 1991. The relative importance of the various nonlinear mechanisms in a wide range of tidal interactions. In: B.B. Parker (ed.), Tidal Hydrodynamics, John Wiley, New York, pp.237–268.

Pawlowicz R., Beardsley, B., Lentz, S., 2002. Classical tidal harmonic analysis including error estimates in MATLAB using T_TIDE. Computers & Geosciences 28, 929–937.

Pingree R.D., Maddock L., 1978. The M_4 tide in the English Channel derived from a non-linear numerical model of the M_2 tide. Deep-Sea Research 25, 52-63.

Postma H., 1961. Transport and accumulation of suspended matter in the Dutch Wadden Sea. Netherlands Journal of Sea Research 1, 148–190.

Pugh D.T., 1987. Tides, surges and mean sea-level, 472 pp., John Wiley, Hoboken, N.J.

Sassi M.G., Hoitink A.J.F., 2013. River flow controls on tides and tide-mean water level profiles in a tidal freshwater river. Journal of Geophysical Research 118, 1–3, doi:10.1002/jgrc.20297.

Savenije H.H.G., Toffolon M., Haas J., Veling E.J.M., 2008. Analytical description of tidal dynamics in convergent estuaries. Journal of Geophysical Research 113, C10025, 1–18, doi:10.1029/2007JC004408.

Stronach J.A., Murty T.S., 1989. Nonlinear river-tidal interactions in the Fraser River, Canada. Marine Geodesy 13(4), 313–339.

Talke S.A., Jay D.A., 2020. Changing tides: the role of natural and anthropogenic factors. Annual Review of Marine Sciences 12, 14.1-14.31.

van Rijn L.C., 2011. Analytical and numerical analysis of tides and salinities in estuaries, part I: tidal wave propagation in convergent estuaries. Ocean Dynamics 61, 1719–1741.

Walters R.A., Werner, R.E., 1991. Nonlinear generation of overtide, compound tides, and residuals. In: B.B. Parker (ed.), Tidal Hydrodynamics, John Wiley, Toronto, pp.297–320.

Wang Z.B., Juken H., de Vriend H.J., 1999. Tidal asymmetry and residual sediment transport in estuaries. WL|Hydraulic, report No. Z2749, 66 pp.

https://doi.org/10.5194/hess-2021-75
Preprint. Discussion started: 26 February 2021

Hydrology and Earth System Sciences
Discussions

Zimmerman J.T.F., 1992. On the Lorentz linearization of a nonlinearly damped tidal Helmholtz oscillator. Proceeding KNAW 95 (1), 127–145.

Zhang E.F., Savenije H.H.G., Chen S.L., Mao X.H., 2012. An analytical solution for tidal propagation in the Yangtze Estuary, China. Hydrology and Earth System Sciences 16, 3327-3339.